

# Scientific program

## 1. Test of the Time Reversal Invariance in Nuclear Reactions with Polarized Neutrons

The source of the CP - violation (which implies time reversal violation via the CPT theorem) is unknown up to now. The CP - violation effect was first observed in the kaon decay only about 35 years ago. Recent  $K_0$  – decay experiment [1] has given direct evidence of the time reversal violation in the elementary – particle phenomena. Nevertheless, searches for the simultaneous parity and time reversal violations in the nonleptonic processes, are still of great importance. The contribution of Kobayashi – Maskawa phase to the corresponding observables is very small. Thus, such experiments probe new types of time reversal invariance violation (TRIV) interactions. At present the study of polarized neutron propagation through polarized targets seems to be one of the most convenient ways to test the time reversal invariance. This is due to the dynamical and resonance enhancement factors, which act in both cases of parity (P - odd) and time reversal violating interactions and cause the increasing of the violation effects near the neutron p – wave resonances.

Neutron transmission is described by the forward neutron-nucleus scattering amplitude:

$$f = A + B(\vec{s} \cdot \vec{I}) + C(\vec{s} \cdot \vec{k}) + D(\vec{s} \cdot [\vec{k} \times \vec{I}]) + E(\vec{s} \cdot [\vec{k} \times \vec{I}]) \cdot (\vec{k} \cdot \vec{I}) \quad (1)$$

Here  $\vec{s}$  is the neutron spin,  $\vec{I}$  is the spin of the target nuclei, and  $\vec{k}$  is the neutron wave vector. The coefficient  $A$  represents the strong, neutron spin independent interaction. The coefficient  $B$  represents the combined effects of external magnetic field, spin - orbit interaction between the neutron and the nucleus, and the interactions of the neutron magnetic moment with nuclear and electron magnetization,  $C$  is the amplitude of weak P - odd interaction. The coefficient  $D$  represents the parity and the time reversal odd scalar - triple product and  $E$  is the P-even T-odd coefficient. The real parts of all coefficients cause a precession of the neutron around the relevant directions and the imaginary parts lead to the attenuation depending on the neutron spin direction.

The effect of the  $D$  term on the neutron transmission should be observable as a transmission difference for the two inverse states of the neutron spin polarizer because the sign of the spin correlation  $\vec{s} \cdot [\vec{k} \times \vec{I}]$  changes. The effect of the  $E$  term can be seen in a transmission experiment with polarized neutrons and aligned target. The three-fold correlation arises from the symmetry of scattering from  $s_{1/2}$ -wave to  $p_{1/2}$ - and  $p_{3/2}$ -waves and vice versa. It is P-odd, as the transitions between s- and p-waves are parity violating. The five-fold correlation tests the equality of the transition rates from  $p_{1/2}$ -wave to  $p_{3/2}$ -one and vice versa, thus it is P-even.

In accordance with nowadays theoretical expectations the ratio  $\lambda = D/C_w$  of the TRIV weak matrix element to P-odd one  $\leq 10^{-4}$ , However, all of them are indirect and the lack of experimental information leads to the conclusion that practically in every class of models this ratio might be large enough to be measured in the neutron transmission experiment [2].

However, as it has been suggested by the consideration of possible experimental designs, there are many fake effects which mask the true TRIV [3]. The most serious effect is due to the pseudomagnetic field which gives rise to a rotation of the neutron spin around the target polarization. It is proportional to  $\text{Re}[B]$  in (1). Besides, the polarization of the neutron polarizer is different from that of the analyzer. This introduces a fake effect into the transmission difference, which is proportional to the difference between the polarizer and analyzer polarizations. Another fake effect arises due to misalignments in the settings of the polarization axes of the polarizer, the analyzer and the target. We intent to realize the experimental technique which has been proposed in [4]. The technique is based on P – A theorem and allows to decrease the systematic contribution of the fake effects below the threshold which is required to measure  $\lambda$  at the level of  $10^{-4}$ . Figure 1

shows the result of Monte Carlo simulation of TRIV effect for the method has been proposed in [4]. The result was obtained for the present KEK LaAlO<sub>3</sub> target of 3×3×3 cm<sup>3</sup>. The conditions of simulation are shown in Table 1.

The second way to test time invariance in the nuclear reactions is the investigation of the elastic scattering of polarized neutrons by zero – spin nuclei [5]. This is possible because of contribution of TRIV interaction to elastic cross section:

$$\frac{d\sigma}{d\Omega} \approx \alpha + 2 \operatorname{Re} \left[ f_0^* \left( f_p (\vec{k}' + \vec{k}) \cdot \vec{s} + f_{pT} (\vec{k}' - \vec{k}) \cdot \vec{s} \right) \right] \quad (2)$$

Here,  $f_0$  is an amplitude of s – wave scattering. The amplitude  $f_p$  corresponds to P – odd interaction, and  $f_{pT}$  corresponds to the simultaneous violation of the space parity and time invariance. It arises due to the same interaction like in forward scattering amplitude (1). The unit vectors  $\vec{k}$  and  $\vec{k}'$  are directed along the momenta of incoming and scattered neutrons respectively. The quantity  $\alpha$  depends on usual strong interaction only.

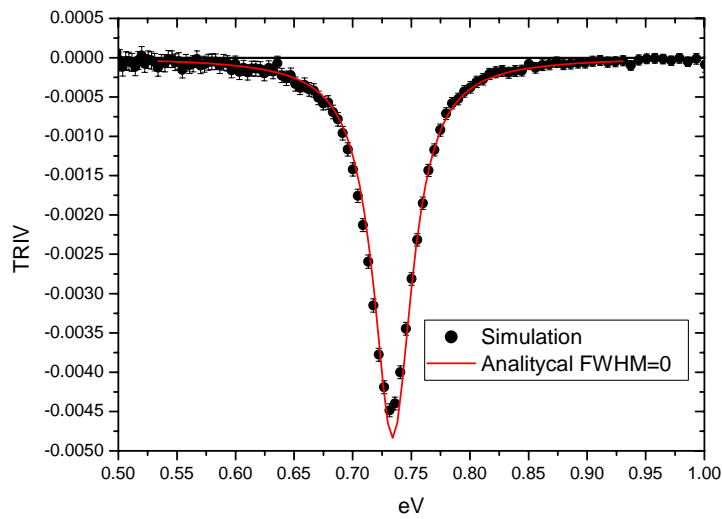


Figure 1. Simulation of TRIV effect in transmission for <sup>139</sup>LaAlO<sub>3</sub>. See text for details.

Table 1

TRIV – matrix element $w_{pT}$	$= w_p = 3.3 \text{ meV}$ [7]*
<sup>139</sup> La polarization $p_t$	0.5
Compensation field	842 Gauss ( 1% - deviation from the optimal one 849 Gauss)
TOF path	15 m
TOF encoder channel width	4 $\mu\text{s}$
Neutron pulse width FWHM	3 $\mu\text{s}$
Neutron detector	<sup>3</sup> He proportional counter (10 atm) 15 cm in length
Neutron polarizer	<sup>3</sup> He (10 atm) with polarization of 0.6

\* To obtain the value of the expected effect one should *multiply* the quantities on figure 1 by the expected ratio of  $w_{pT} / w_p$ .

We see that for the backward scattering  $\vec{k}' = -\vec{k}$ , the contribution of P – odd term disappears. Thus, the presence of TRIV amplitude  $f_{pT}$  may be detected if one measure the backward scattering rate difference for two opposite neutron spin states.

This result may be easily understood. In backward scattering, the projections of the neutron orbital momenta both in the entrance and exit channels on the  $\vec{k}$  direction are zero. Thus, when the nuclear spin  $I = 0$  the spin direction for longitudinally polarized neutron is conserved. In the general

case of  $I \neq 0$ , the projection of the neutron spin on the  $\vec{k}$  direction may change due to the combined flip of the neutron and nuclear spins. Thus, due to the conservation of neutron spin direction, backward scattering by a zero spin nucleus of the right – polarized neutron is the time-reversal of the same process for the left – polarized one. To see that, it is necessary to reverse the directions of the momenta of the incident and scattered neutrons and their spins, and then replace the initial and final states of the process. If time invariance holds, then the probabilities of backward scattering by zero spin nuclei of the left – and right – polarized neutrons should be equal. Thus, the asymmetry of backward scattering by zero spin nuclei of neutrons with opposite helicities would evidence time invariance breaking. One should note that the backward asymmetry may exist for non-zero spin nuclei due to space parity violation, but generally it is not related with time - invariance breaking.

The scattering experiment obviously does not require polarized target, but it is less efficient than the transmission one. Namely, because of much less count rate. Thus, the statistics will be smaller. This type of experiment may set just the limit for  $\lambda$  at the level of  $\sim 10^{-2}$ . Nevertheless, it allows the simultaneous test of the time reversal invariance in a wide range of p – wave resonances. Figure 2 shows the result of Monte Carlo simulation of the net TRIV effect in a backward elastic scattering of the longitudinally polarized neutrons on  $^{232}\text{Th}$ . The effects are shown in the vicinity of p – wave resonances of 36.97 and 38.19 eV in assumption that  $w_{PT}$  are equal to the corresponding  $w_P$ . The other parameters have been used for simulation are shown in Table 2.

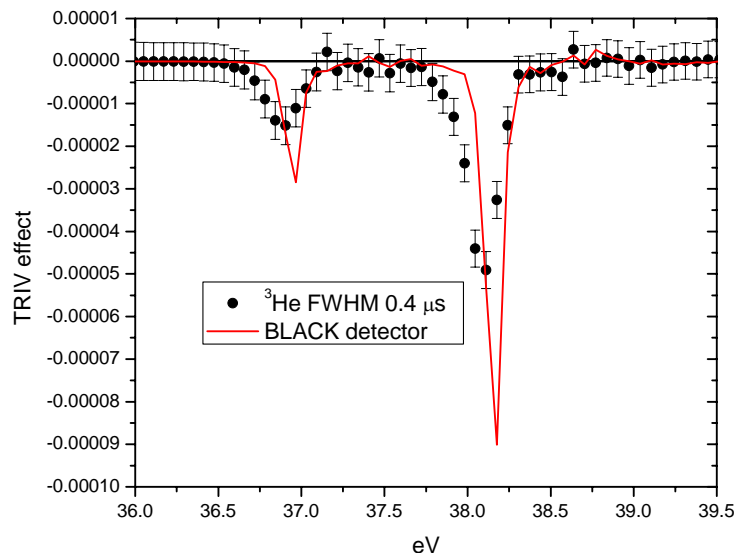


Figure 2. Simulation of TRIV effect in elastic scattering for  $^{232}\text{Th}$ . See text for details.

Table 2.

TRIV – matrix element $w_{PT}$	$= w_P = 1 \text{ meV}$
Neutron beam polarization	0.5
TOF path	50 m
TOF encoder channel width	$0.5 \mu\text{s}$
Neutron pulse width FWHM	$0.4 \mu\text{s}$

The curve is marked as “black” corresponds to the case of an ideal detector with the efficiency of registration of 100% and  $\text{FWHM} = 0$ .

One should note, that the most of models assume no correlation between the magnitudes of the  $w_{PT}$  and  $w_P$  matrix elements. It means, that effect has shown in figure 2 may be smaller and bigger as well. Thus, the assumption of  $w_{PT} = w_P$  is artefact in some sense and has been chosen just for demonstration purpose.

## References

1. A. Angelopoulos et al., Phys. Lett. B 444 (1998) 43.
2. Gudkov V.P. In Parity and Time Reversal Violation in Compound Nuclear States and Related Topics, (World Scientific, Singapore, 1996) 231.
3. R. Golub, S.K. Lamoreaux, Phys. Rev. D 50 (1994) 5632.
4. V.R. Skoy, Phys. Rev. D 53 (1996) 4070.
5. A.L. Barabanov and V.R. Skoy, Nucl. Phys. A 644 (1999) 54.

## 2. Neutron mean square charge radius and electric polarizability

In spite of long standing and numerous attempts to obtain the experimental estimates of the neutron mean square charge radius  $\langle r_n^2 \rangle$  and neutron electric polarizability  $\alpha_n$ , these values are known with accuracy not better 30 % and 100%, respectively. The reason of this is the corrections, which are of the same order or even larger than the searched effects amounted to  $10^{-4} - 10^{-2}$  of the nuclear cross sections. Besides, the n,e-scattering length  $b_{ne}$ , from which the  $\langle r_n^2 \rangle$  value is derived, has two groups of experimental data near  $-1.32 \cdot 10^{-3} \text{ fm}$  and  $-1.60 \cdot 10^{-3} \text{ fm}$  which differ by  $\sim 10$  statistical errors. The  $\langle r_n^2 \rangle$  has the following relation with  $b_{ne}$

$$\langle r_n^2 \rangle = \frac{3\hbar^2}{M_n e^2} b_{ne}.$$

As for recently obtained with a good accuracy  $\alpha_n$  value from measurements with deuterons, it is certainly model dependent and therefore it does not exclude the necessity of the direct measurements of  $\alpha_n$  with free neutrons.

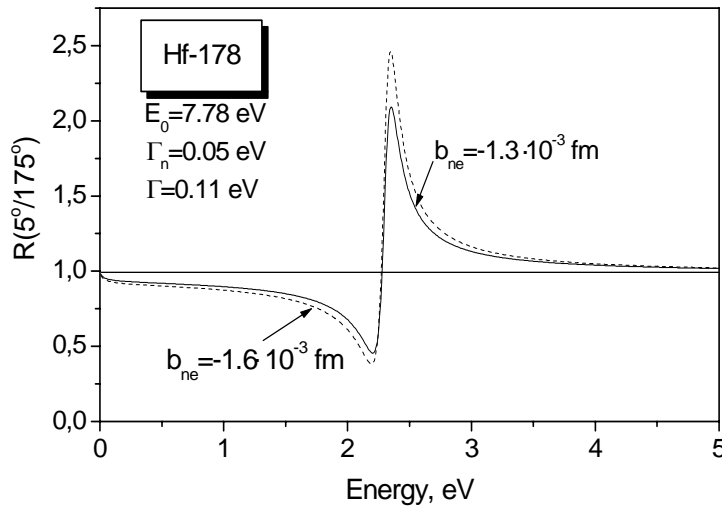


Fig.1. The forward-backward ratio of intensities of scattered by  $^{178}\text{Hf}$  neutrons near the resonance with  $E_0 = 7.78 \text{ eV}$ .

The continuation of investigations on  $b_{ne}$  and  $\alpha_n$  are planned at IREN using specific properties of s-wave neutron resonances. Such a resonance with energy  $E_0$  for even-even nucleus makes a deep minimum of the scattering cross section at  $E^* = E_0 - \frac{\Gamma_n}{2kR'}$  ( $R'$  is the scattering radius,  $k$  and  $\Gamma_n$  are the resonant values of the neutron wave number and neutron width), where the

real part of the total scattering amplitude intersects the abscissa axis. As a result, its interference term with  $b_{ne}$  changes its sign at  $E = E^*$  and this allows to get  $b_{ne}$  from a measurement of the forward-backward ratio of the scattering intensity. Fig.1 demonstrates such a ratio in case of  $^{178}\text{Hf}$  resonance for two  $b_{ne}$  values. But to use this theoretical huge effect in practice is not so easy due to necessity to have a very pure isotope sample.

Another application of resonance minima is shown in Fig.2 where the intensity of neutrons transmitted through a 15–20 cm thick  $^{238}\text{U}$  filter is given. This picture can be sufficiently extended with quasi-monochromatic “lines” in the interval from 2 to 140 keV using the given by Nature elements *Sc, Al, Fe, Si* etc. The beam of these “lines” together with the time-of-flight technique allows to execute a variety of experiments practically without background. And the first of them is the precise measurement of the total cross section for  $^{208}\text{Pb}$  in order to estimate the  $\alpha_n$  value.

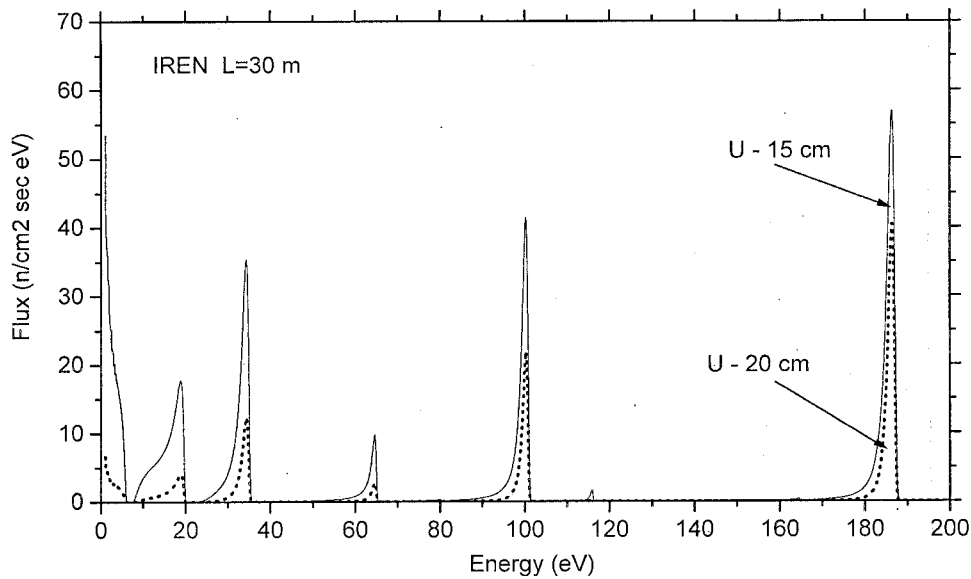


Fig.2. The neutron flux at IREN at  $L = 30\text{ m}$  flight path after a 15–20 cm thick  $^{238}\text{U}$  filter.

The “line” 6.52 eV (the lowest energy in Fig.2) can be used for the  $b_{ne}$  estimation by means of forward-backward ratio observation which is presented in Fig.3.

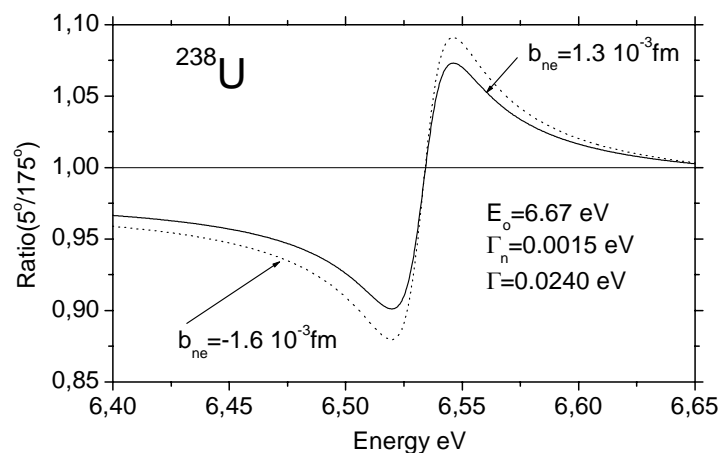


Fig.3. The forward-backward ratio of intensities of the scattered by  $^{238}\text{U}$  neutrons near the resonance with  $E_0 = 6.67\text{ eV}$ .

Last, but not least, a very promising experiment for IREN with the minimum and clear corrections is the measurement of transmission of gaseous isotope  $^{86}\text{Kr}$  at different pressures (1-50 atm) in a broad energy interval ( $\sim 10 \text{ meV} - 24 \text{ keV}$ ). The total cross section of  $^{86}\text{Kr}$  has a form

$$\sigma_{tot} = \sigma_s \left( 1 + 8\pi \frac{b_{Ncoh} b_{ne}}{\sigma_s} Zf(E) + P \frac{Const}{E} \right) + \sigma_{ny}.$$

The term proportional to pressure  $P$  is caused by the neutron diffraction on pairs of the neighbouring atoms; it can exceed the term with  $b_{ne}$  by 5 – 10 times at  $P \approx 50 \text{ atm}$ . The capture cross section is negligibly small ( $\sigma_{ny} \approx 3 \text{ mb}$  at  $E \approx 25 \text{ meV}$ ).

Fig.4 demonstrates the possibility to derive  $b_{ne}$  not much depending on the calculated electron form-factor  $f(E)$ , integrated over angles. It is necessary to know exactly the “shoulders” of the picture:  $\sigma_{tot}$  at  $E > 200 \text{ eV}$  where  $f \cong 0$  and  $\sigma_{tot}$  at  $E \rightarrow 0$  where  $f \cong 1$ . Moreover, in order to know the nuclear amplitude behavior at  $E < 200 \text{ eV}$ , the  $\sigma_{tot}$  value has to be measured in a possibly broader energy interval.

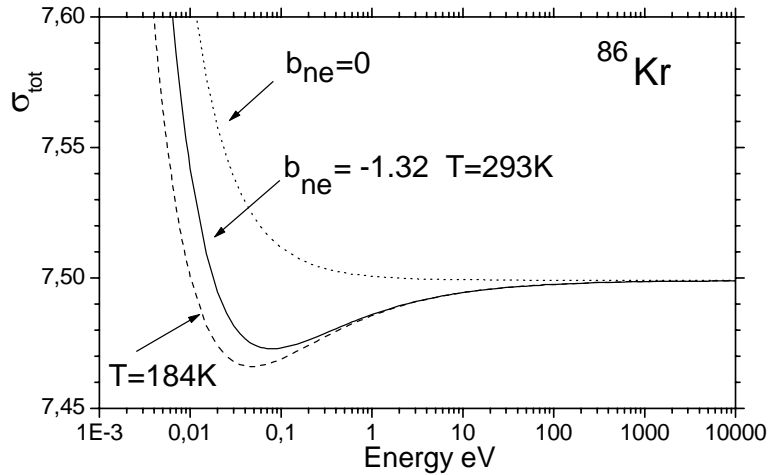


Fig.4. The  $\sigma_{tot}(E)$  of  $^{86}\text{Kr}$  at different gas temperature.

The necessary precision  $10^{-4}$  will permit not only to determine quite weighty contribution (1%) of the n,e-scattering but also to certify with the same accuracy the adequateness of the nuclear scattering description by the widely used R-matrix formalism and by its limiting case one-level Breit-Wigner approximation. Getting accuracy estimates of description of the neutron cross section structure in resonance region by the modern models has an independent scientific value.

### 3. The IREN + UGRA experiments

A number of rather different experiments are planned with the UGRA scattered neutrons spectrometer [1-3] situated at the 250 m time-of-flight path. It allows to measure the neutron spectra at energies between several eV and  $\sim 100 \text{ keV}$ . The scheme of the instrument is shown in Fig.1. Up to 16  $^3\text{He}$ -detectors are placed in a big ( $\sim 3 \text{ m}$ ) aluminum vacuum chamber on a rotary platform, so each detector can count scattered neutrons at nine angles from  $25^\circ$  to  $155^\circ$  from one of three scatterers attached on a special holder in the chamber center.

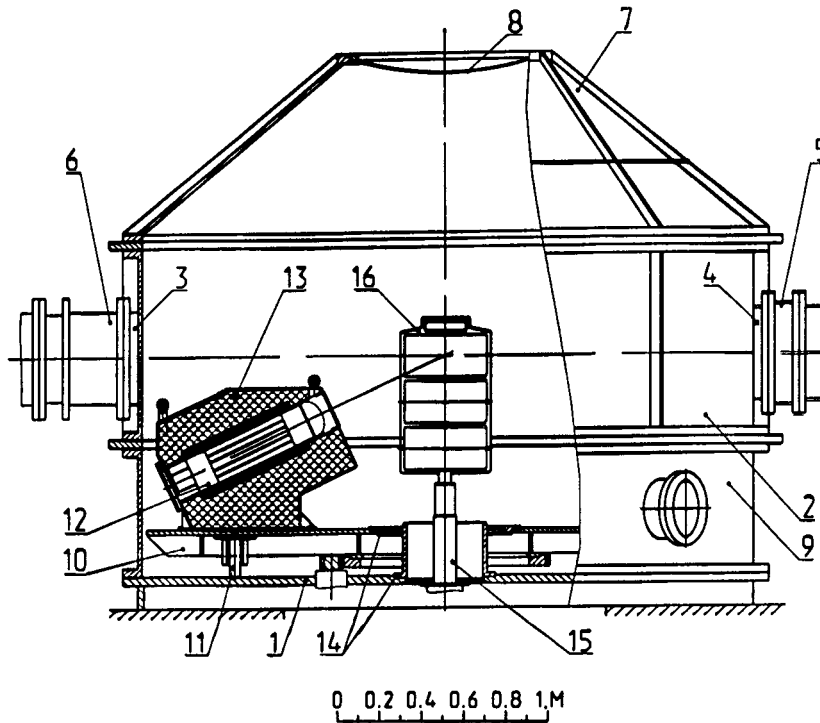


Fig.1. Arrangement of the UGRA spectrometer. 1 - chamber bottom; 2 - middle section; 3,4 - sleeves for connections with neutron beam-tubes; 5- bellows; 6- temperature compensator; 7- upper section; 8 - membrane; 9 - lower section; 10- rotary platform; 11 -wheels for rotary platform; 12 - neutron detector; 13 - shielding tank; 14- centralizing device; 15 - vertical rod; 16 - sample holder.

An obtained angular distribution should be presented in the form

$$I(\vartheta) = C[1 + \omega_1 \cos \vartheta + \omega_2 P_2(\cos \vartheta)], \quad (1)$$

if it is measured at three or more angles  $\vartheta$ . The  $I(\vartheta)$  function and  $C$  constant can be replaced in (1) by the differential scattering cross section  $d\sigma/d\Omega$  and  $\sigma_s/4\pi$  ( $\sigma_s$  is the total scattering cross section), if an additional measurement has been made on nuclei with the known  $\sigma_s$ .

### 3.1 The neutron electric polarizability $\alpha_n$ .

There is a possibility to get a new estimation of the  $\alpha_n$  value if precise  $d\sigma/d\Omega$  cross section is obtained at neutron energies  $E \sim 1 - 100$  keV for the heavy nuclei ( $Z > 72$ ) which possess good resonance averaging, and which are accessible for making massive elementary scatterers. The forward-backward asymmetry coefficient  $\omega_1(E)$  contains a small specific contribution proportional to  $\alpha_n Z^2 E^{1/2}$  on the background of pure nuclear contributions  $\sim E$ ,  $\sim E^{3/2}$  and  $\sim E^2$  defined by the scattering radii and strength functions for s- and p-neutrons. A combined analysis of  $\omega_1(E)$ ,  $\omega_2(E)$ ,  $\sigma_s(E)$  with possible addition of some data on the total and  $(n, \gamma)$  cross sections will allow to determine all parameters including  $\alpha_n$  [4].

There are very good prospects for investigations of little known and unknown properties of the individual resonances too. For this aim, the resonance areas will be measured at different scattering angles  $\vartheta$  and fitted by the expression (1).

### 3.2 The spin channel mixtures.

A p-wave resonance with the total spin  $J = I \pm 1/2$  ( $I$  is the target – nucleus spin) is excited and decays through two channels with the spins  $s = I \pm 1/2$  (see [5] for example):

$$\bar{J} = \bar{I} + \frac{\bar{I}}{2} + \bar{I} = \begin{cases} I+1/2+0 \\ I-1/2+1 \\ I+1/2-1 \\ I-1/2+0 \end{cases} = \begin{cases} I+1/2 \\ I-1/2 \end{cases}$$

So, for such resonance the neutron width  $\Gamma_n = \Gamma_- + \Gamma_+$  is the sum of two widths, and the  $\omega_2$  value in (1) depends on the mixture of  $\Gamma_-$  and  $\Gamma_+$ , for example on parameter

$$\beta = \Gamma_- / (\Gamma_- + \Gamma_+). \quad (2)$$

The  $\omega_2(\beta)$  is a squared function of  $\beta$  and pictured by a parabola which touches the abscissa axis somewhere between  $\beta = 0$  and  $\beta = 1$  depending on  $I$  and  $J$ . Fig.2 shows an example of  $\omega_2(\beta)$  for  $I = 1/2$  and  $J = 1$ . Only one value of  $\beta$  corresponds to the given value of  $\omega_2$  for the case when  $0.5 < \omega_2 \leq 2$ . But if an experiment gives  $\omega_2 \leq 0.5$ , then  $\beta$  can have any of two possible values.

The knowledge of  $\beta$  is necessary in the investigations of parity nonconservation effects at the mixed s- and p-wave resonances. This is very useful for the test of nuclear statistical model in search for the partial width correlations. At last, without knowledge of  $\beta$  we poorly know the angular dependence of neutron scattering which is necessary for practical purposes.

Up to now, the  $\beta$  value has been measured only for 18 p-wave resonances for 7 target-nuclei [5]. But in 4 cases, for resonances of  $^{89}\text{Y}$ , two possible  $\beta$  have been obtained.

### 3.3 The mixed (s+d)-wave resonances.

Theoretical investigation of this subject in details is presented in [6] and all what we mention below is based on this work.

The areas of an s-wave resonance for different angles  $\vartheta$  should be analyzed with the expression (1) which has to be completed by the term  $\omega_4 P_4(\cos \vartheta)$ . The observation of nonzero  $\omega_4$  and (or)  $\omega_2$  means definitely the admixture of d-wave to s-wave in such resonance. Moreover, if spins  $I \geq 3/2$  and  $J \geq 2$  then both spin channels are open for the d-wave neutrons and the neutron width consists of three parts:

$$\Gamma_n = \Gamma_s + \Gamma_{d-} + \Gamma_{d+}.$$

So, the mixed resonances are characterized by two mixture parameters: for the orbital channels

$$\alpha = \frac{\Gamma_{d-} + \Gamma_{d+}}{\Gamma_s + \Gamma_{d-} + \Gamma_{d+}} \quad (3)$$

and spin channels (like (2) for the p-wave resonances)

$$\beta = \frac{\Gamma_{d-}}{\Gamma_{d-} + \Gamma_{d+}}. \quad (4)$$

Both parameters (3), (4) can be found (as single-valued or having two or three possible values) from the experimental data on  $\omega_2$  and  $\omega_4$  with the help of the formulae:

$$\omega_2 = \begin{cases} [\alpha(a\beta + b) \pm 2\sqrt{\alpha(1-\alpha)\beta} \cos(\delta_0 - \delta_2)]^2 & \text{for } J = I - 1/2 \\ [\alpha(a\beta + b) \mp 2\sqrt{\alpha(1-\alpha)(1-\beta)} \cos(\delta_0 - \delta_2)]^2 & \text{for } J = I + 1/2 \end{cases}, \quad (5)$$

$$\omega_4 = [\alpha(c\beta + d)]^2,$$

where  $\delta_0$  and  $\delta_2$  are the phase shifts for s- and d-wave potential scattering, the constants  $a, b, c, d$  are given in [6] for the whole set of  $I, J$ .



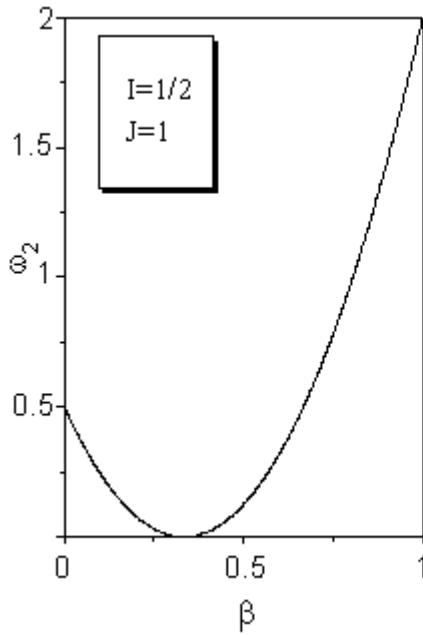


Fig.2. Dependence of  $\beta$  on  $\omega_2$  for  $I=1/2$ ,  $J=1$ .

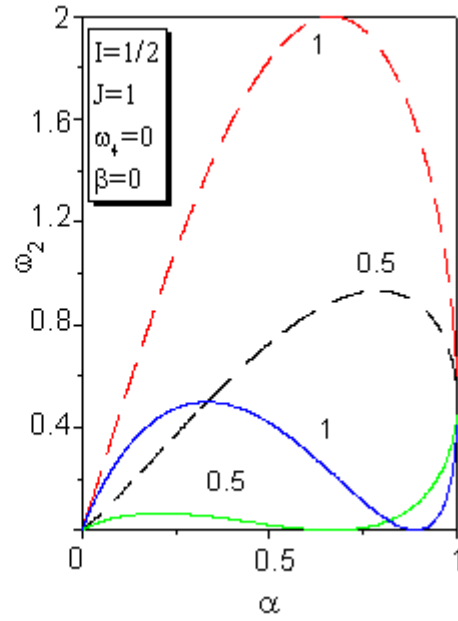


Fig.3. Scattering anisotropy at resonances for nuclei with  $I=1/2$ . Numbers near lines – values  $\cos(\delta_0 - \delta_2)$ . Solid lines – for equal signs of amplitudes, dashed lines – for different ones.

Two expressions (5) allow to get the unique information for neutron spectroscopy about the relative signs of partial width amplitudes  $\gamma_i = \pm\sqrt{\Gamma_i}$  for the pair  $\Gamma_s$  and  $\Gamma_{d-}$  or  $\Gamma_s$  and  $\Gamma_{d+}$ . The upper signs in (5) correspond to the same signs and the under – to opposite ones.

The simplest example in the case of a nucleus with  $I = 1/2$ ,  $J = 1$  is shown in Fig.3. Such a resonance has  $\omega_4 = 0$  and no spin channels mixture. The solid curves correspond to the same amplitude signs and the dashed ones – to the opposite signs. The numbers 0.5 and 1 at curves are the values of  $\cos(\delta_0 - \delta_2)$ . It is obvious that if an experiment gives  $\omega_2 > 0.5$  then  $\sqrt{\Gamma_s \cdot \Gamma_d} < 0$  and there are two possible quantities for  $\alpha$ . If  $\omega_2 < 0.5$  then the  $\sqrt{\Gamma_s \cdot \Gamma_d}$  sign is uncertain and  $\alpha$  can have any of two or even three values.

The mixed (s+d)-wave resonances are not rare at the neutron energies  $E \sim 1$  MeV or higher. About 20 such resonances are known at  $E \sim 180 - 600$  keV (see references in [6]). Due to the centrifugal barrier, the observation of such a resonance at  $E \sim 10 - 100$  keV is improbable and would be an interesting uninvestigated nonstatistical effect in a compound-nucleus.

### 3.4 The thermal motion effect on resonance scattering.

As it is known (see for example [7]), the neutron cross section at energies  $\sim$  eV and lower are formed with participation of the thermal motion of atoms in the sample. This exhibits in the well-known Doppler broadening of the neutron resonances. Moreover, there are some considerations [8] that the thermal motion in substance can influence on the angular dependence of neutron scattering in a resonance. This effect was never observed and never calculated yet. Thus, the isotropic in the center-of-mass system scattering in an s-wave resonance can become nonisotropic. Then its parameters  $\omega_1$  and  $\omega_2$  in (1) in the laboratory system will differ from  $2/A$  and  $1/A^2$  ( $A$  is mass number), which they are at the isotropy in

the center-of-mass system. The experiments should be carried out with the pure s-wave resonances at eV energies.

#### References.

1. Б.И.Воронов, Т.Л.Еник, В.А.Ермаков, В.И.Константинов, Е.И.Литвиненко, Л.В.Мицына, Г.С.Самосват, А.А.Смирнов, В.А.Трепалин, Р.В.Харьюзов. Сообщение ОИЯИ Р13-97-36, Дубна, 1997.
2. Т.Л.Еник, Л.В.Мицына, Г.С.Самосват, А.А.Смирнов, Р.В.Харьюзов. Сообщение ОИЯИ Р13-97-372, Дубна, 1997.
3. T.L.Enik, R.V.Kharjuzov, L.V.Mitsyna, G.S.Samosvat. Nucl. Instr. Meth. A, **440**(2002),777.
4. Ю.А.Александров, Г.С.Самосват. В кн.: VI Международная школа по нейтронной физике, ОИЯИ Д3, 14-91-154, Дубна, 1991, т.1,187.
5. Г.С.Самосват. ЭЧАЯ, **26**(1995), в.6,1567.
6. Л.В.Мицына, Г.С.Самосват. Сообщение ОИЯИ Р3-90-234, Дубна, 1990.
7. С.Б.Шихов, В.Б.Троянский. Теория ядерных реакторов, Энергоатомиздат, Москва, 1983.
8. А.А.Лукьянов. Частное сообщение.

#### 4. Search for possible long-range van der Waals interaction between neutron and nucleus

A possibility of the existence of a long-range component in the strong interaction between hadrons was discussed previously using different approaches. Some theoretical aspects of strong long-range interaction between hadrons were analyzed by many authors (see for example the review [1] and references therein) without any final firm conclusion about existence and strength of these forces. It was concluded that existence of such forces is not impossible, the most plausible mechanism for generating long-range strong potential is multi-gluon exchange.

Experimental situation concerning strong long-range forces between hadrons was also discussed in [1]. It turned out that if to parametrize these potentials in the form  $U(r) = c(1 \text{ fm}/r)^n$  the most stringent restriction followed from the measurements of radiative transitions in anti-protonic atoms:  $c \leq 100 \text{ MeV}$  ( $n=6$ ), and  $\leq 600 \text{ MeV}$  ( $n=7$ ). Similar bounds on the value of these potentials follow from transitions in pionic atoms. Other experiments (Cavendish or Eötvös-type experiments, hyperfine structure of molecular hydrogen) give much weaker bounds on long-range potentials with  $n=6$  or 7.

Irrespective of theoretical predictions which are very indeterminate, the bounds on the magnitude of this interaction may be obtained from experiments involving a variety of techniques.

If such interaction really exists some signals of it could be found in neutron-nuclei interaction. Possible hint on existence of strong long-range neutron-nucleus interaction comes from experiments on the search for neutron polarizability. In a series of experiments and careful optical model calculations, the authors of [2] showed that the great variety of data on neutron scattering in MeV energy range (total cross sections, angular distributions and especially small angle scattering) have better description (in the sense of  $\chi^2$  value) if, in addition to the short-range Woods-Saxon potential of general form and the Schwinger interaction, the neutron electric polarizability term with the factor as large as  $\alpha_n \cong (1 - 2) \cdot 10^{-1} \text{ fm}^3$  is included into the potential of neutron-nucleus interaction. This value of the neutron electric polarizability is two orders of magnitude higher than the value expected from reasonable calculations and the several measurements by different groups in keV neutron energy range. It might be possible, as was proposed in [3], that some other potential of the  $\sim r^{-n}$  type with  $n>4$ , for example with  $n=6$  (Van der Waals), or  $n=7$  (Casimir-Polder) influences neutron scattering in the MeV energy range.

The scattering amplitudes in the first Born approximation for  $n=4-7$  generally behave similarly in the range  $x=qR < 5$  ( $q$  is wave vector transfer at scattering,  $R$  is nuclear radius) where the amplitudes are not small, differing only by the factor which does not change significantly. The same is true for the several first Born scattering phases for these potentials in MeV neutron energy range. It means that it is possible that large potential of the  $r^{-4}$  type inferred from fast neutron scattering [2] may be in fact the potential  $r^{-n}$  with  $n=6$  or  $n=7$  but of correspondingly larger magnitude at  $r=R$ .

The optical model calculations of differential cross sections of neutron scattering on heavy nuclei in the energy range 0.5-10 MeV [4] demonstrated that the effects of additional long-range potentials with  $n=4-7$  on neutron cross sections are very close if to fit appropriately the value  $U_R$  of the potentials at nuclear boundary. For example the value  $U_R \cong 200$  keV for the neutron polarizability potential inferred from experiments [2] must be changed to  $U_R \cong 300$  keV for the long-range potential with  $n=6$  to achieve close similarity of their effects on cross sections with difference in the limits of several per cent.

Experiments on neutron-nuclei scattering in thermal energy range (as well as neutron optics experiments) are very insensitive to these potentials. With  $U_R=300$  keV and neutron energy  $E_n=100$  meV it follows from above expression that the contribution of the term  $x^3$ , specific for van der Waals potential, is  $\cong 10^{-10}$  of the neutron-nucleus amplitude.

Better confirmation or more strict constraints for the existence of strong long-range neutron-nucleus interaction requires detailed computations with the most flexible nuclear optical potential and inclusion of long-range potentials of the  $r^{-n}$  type with different  $n$ . This complicated procedure must establish what kind of a long-range potential is able to satisfy better the description of the whole set of data on fast neutron-nucleus scattering.

Besides this approach used in [2] to infer the long-range contribution to neutron-nucleus interaction, two ways are possible to determine the long-range potential explicitly using the characteristic  $k$  dependence of the scattering amplitude described above. Both follow from the long search for the electric polarizability of the neutron. One way is the very precise measurement of angular distribution, the second one - the measurement with millibarn precision of total cross sections of neutron scattering by different (light and heavy) nuclei in the energy range up to several hundred keV. No such data are available now.

We propose to perform careful precision (2-5 mb) measurements of total neutron cross section for several light and heavy nuclei (C, O,  $^{208}\text{Pb}$ ) in the neutron energy range 1-100 keV. The parameters of the IREN neutron source are appropriate for this task as follows from previous measurements of the neutron total cross sections at the IBR-30 complex [5].

In view of importance of this question for the theory of strong interaction it is worthwhile pursuing it, as well as finding more crucial experiments for distinguishing strong long-range component in nucleon-nucleon and nucleon-nucleus interaction.

## References

- [1] G. Feinberg and J. Sucher, Phys. Rev., D20 (1979) 1717.
- [2] G.V. Anikin and I.I. Kotukhov, Jad. Fiz., 12, 1121 (1970); G.V. Anikin and I.I. Kotukhov, Jad. Fiz., 14, 269 (1971); G.V. Anikin and I.I. Kotukhov, Atomnaja Energija., 60, 51 (1986); G.V. Anikin and I.I. Kotukhov, Atomnaja Energija., 60, 54 (1986); G.V. Anikin and I.I. Kotukhov, Proc of the Ist Intern. Conf. on Neutron Physics, Kiev, 14-18 Sept. 1987, Vol.2, p.139; G.V. Anikin and I.I. Kotukhov, Jad. Fiz., 49, 101 (1989); I.I. Kotukhov, Dissertation, Fiziko-Enegeticheskii Institute, Obninsk, 1990, (in Russian, unpublished).
- [3] Yu.N. Pokotilovski, JINR Preprint E4-99-135, Dubna, 1999; Proc. of the VII Intern. Seminar on Interaction of Neutrons with Nuclei, Dubna, May 25-28, 1999, p.308.

[4] S.V. Konnova, V.V. Lyuboshits, and Yu.N. Pokotilovski, Proc. of the VII Intern. Seminar on Interaction of Neutrons with Nuclei, Dubna, May 25-28, 1999, p.325.

[5] T.L.Enik et al, Jad. Fiz., 66, 59 (2003).

## 5. Study of quantum features of fission by resonance neutrons

Study of nuclear fission induced by slow neutrons from its discovery provides a lot of essential information on properties and nature of this phenomenon. In spite of long history of such research up to now neutrons remain very fruitful tool to investigate deeper basic properties of nuclear fission.

Special role belongs to resonance neutrons which allows one to study fission proceeding via distinct highly excited states of fissioning nucleus ( compound-states or neutron resonances). For many case spin  $J$  and parity  $\pi$  of such states could be established so it became possible to study this process in very clear conditions. High resolution of TOF neutron spectrometers permits to investigate typical quantum effects such as interference in the total and differential cross-sections of (n,f)-reaction. These effects are very sensitive to shape symmetry of fissile nucleus at scission or more general to properties of wave function of fissioning nucleus on its "way" in deformation "space". A discovery of interference effects in the total (n,f) fission cross-section lead A. Bohr to his concept of transition states which could play role of effective fission channels characterized by fixed values  $J\pi K$  where  $K$  denotes the projection of spin onto the deformation axis of the fissioning nucleus. Recently the conception of transition states was generalized (Barabanov-Furman) to describe the fissioning nucleus on the whole way from the entrance "fission channel" at deformation close to the ground state one ( $\beta_0$ ) up to scission where the system has very large deformation ( $\sim 3\beta_0$ ).

If, as in case of the IREN source, high neutron energy resolution is combined with high intensity it becomes possible to study the influence of nuclear shell effects on the formation of fission barriers and clustering of precission configurations. These phenomena, so called fission modes, extensively investigated during last decade provide in principle very important information on shell structure of nuclei at very large deformations. Indeed wide and rather peculiar mass distribution of fission products realizes some kind of scanning of the genealogical expansion of fissioning nucleus wave function at scission. In these terms distinct fission modes correspond to distinct precission shell configurations that are separated at so called bifurcation points of trajectories in many dimensional deformation space. Some trajectories lead to symmetric fission modes, other give rise to asymmetric fission modes. For different modes second fission barriers could be different. In case of resonance neutron induced fission there is a unique possibility to study fission modes and respective fission barriers for fixed (and known) quantum numbers  $J\pi K$ . It is clear that in such situation one could study the interconnection between A. Bohr's fission channels and fission mode. To realize such program we have to study variation of mass&TKE distributions of fission products with neutron energy.

Besides that there exists another very attractive opportunity to study parity dependence of fission barriers as well as shape symmetry of fissioning nucleus at scission with aid of measuring of neutron energy dependence of interference effects in the differential (n,f) cross-sections. Series of experiments realized at IBR-30 before its final shut-down reveals that  $P_{\text{even}}$  and  $P_{\text{odd}}$  interference of s-wave and p-wave neutron induced fission could be measured with necessary accuracy. Analysis of these measurements provided unique information on characteristics of p-wave fission amplitudes inaccessible for other methods. But low energy resolution of IBR-30 n-TOF spectrometer does not allow to obtain large enough set of p-wave resonance parameters necessary for accurate determination of characteristics of respective fission barriers.

So future experiments at IREN neutron beams provide unique possibility to study various aspect of nuclear fission in very clear conditions. To realize such program it is necessary to improve essentially the DAQ systems as well as fission product detectors.

## 6. Practical investigation of the transformation process of nuclear low-lying levels into the bohr's compound states

Nuclear properties in the excitation interval up to the neutron binding energy  $B_n$  undergoes radical change: the simplest low-lying levels transform into the Bohr's compound states. According to a number of experimental and theoretical works, neutron resonance (compound state of a nucleus) has extremely complicated structure of wave function. On the other hand, structure of low-lying levels is very simple. It is of interest to understand the process of this transformation in the excitation energy interval from  $\cong 5$  to  $\cong 10$  MeV. Understanding of the process occurring in a nucleus and precise calculation of such important for practice parameters as cross-sections of neutron interactions with nuclei require detailed study of this processes in wide mass region and excitation energy interval. This process can be also interpreted as the transition of nuclear matter from "order" to "chaos". At present, the best possibility to know its details is experimental investigation of the two-step gamma-cascades proceeding between the neutron resonance ( $B_n$ ) and group of low-lying levels ( $E_f, E_g, \dots$ ) through all available according to the nuclear selection rules intermediate levels ( $E_i$ ). Fig. 1 demonstrates the idea of the method and gives an example of the results obtained for concrete nucleus.

The developed in FLNP method for analysis of these data provides information on nuclear properties almost over the whole excitation energy interval  $E_{ex} \cong B_n$ . The level density  $\rho(J^\pi, E_{ex})$  and mean partial radiative widths  $\langle \Gamma_{\lambda i}(E_\gamma) \rangle$  of transitions to the states with the excitation energy  $E_i$  contain main information on the wave functions of the studied states. Therefore, the experiment should be aimed at obtaining the maximum complete, precise, and reliable data on  $\rho(J^\pi, E_{ex})$  and  $\Gamma_{\lambda i}$  in maximally wide interval of the excitation energy of any nucleus. Unique possibility for a simultaneous estimation of  $\rho$  and radiative strength functions  $k = \langle \Gamma_{\lambda i} \rangle / (E_\gamma^3 \times A^{2/3} \times D_\lambda)$  of dipole transitions was provided by the study of the cascade of two successive  $\gamma$ -transitions following thermal neutron capture. Using high efficient HPGe detectors one can measure intensity of the individual cascade connecting three states  $\lambda \rightarrow i \rightarrow f$  up to the energy  $E_i \cong 3-5$  MeV, as well as the total intensity of cascades

$$I_{\gamma\gamma} = \sum_{J,\pi} (\Gamma_{\lambda i} / \langle \Gamma_{\lambda i} \rangle m_{\lambda i}) \times n_{\lambda i} \times (\Gamma_{if} / \langle \Gamma_{if} \rangle m_{if})$$

in any energy interval  $E$  of cascade intermediate levels. The mean partial widths  $\langle \Gamma_{\lambda i} \rangle$ ,  $\langle \Gamma_{if} \rangle$ , the total numbers  $m_{\lambda i}$ ,  $n_{\lambda i}$  and  $m_{if}$  of levels excited by E1 and M1 transitions after the decay of the states  $\lambda$  and  $i$ , respectively, can be determined (as it was for the first time ascertained in Dubna) by means of this relation and from experimental values of the total radiative width of the compound state  $\Gamma_\lambda$ . It should be noted that any model ideas of  $\rho$  and  $k$  are not required in this method. For all experimental data obtained up to now, this provides narrow enough intervals of the most probable  $\rho$  and  $k$  for any (including fissile) nuclei. An example of such data for the most precise experiment is shown in Fig.2.

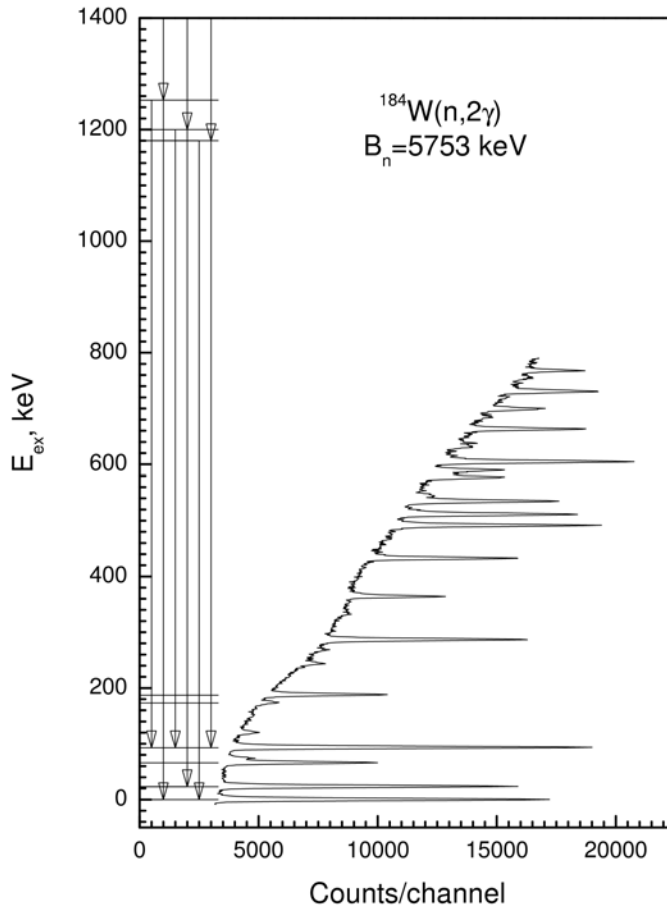


Fig.1. The part of the scheme of excited levels for  $^{185}\text{W}$  (left) and fragment of the sum coincidence spectrum obtained in the experiment (right).

For thermal neutron capture it was established for more than 40 nuclei from the region  $40 \leq A \leq 200$  that the energy dependence of level density is not smooth. Like in Fig.1, level density in these nuclei in the excitation energy intervals from 1-2 to 3-4 MeV (in dependence on parity of nucleon number) is almost constant. At the higher excitation energy, the smallest discrepancy between the experimental and model values of  $\rho$  are observed for the generalized model of superfluid nucleus in the framework of the adiabatic approach.

There are numerous indications that this dependence is step-like at excitation energy above 2-3 MeV contrary to most of the existing theoretical approaches. Respectively, the phonon dipole radiative strength functions could not be consistently described by any modern theoretical models. As it is seen from Fig.2, main discrepancy between the experiment and different model variants of extrapolation of cross-section of reverse reaction ( $\gamma, n$ ) in its sub-threshold energy region consists in difference of shape of dependence on the  $\gamma$ -quantum energy. The value of the discrepancy is lying out of limits of possibility of variations of model parameters.

The general, although clearly qualitative explanation of the observed discrepancy between the experimental and model calculated  $\rho$  and  $k$  values can be obtained from the fact of "non-statistical" behavior of spacing between intermediate levels of the most intense two-step gamma-cascades. For all nuclei under investigation quasi-equidistant "bands" of levels connected with most intense transitions were observed. Besides, in the first approach the values of the most probable equidistant period are proportional to the number of boson pairs in the unfilled nuclear shells. The hypothesis of vibrational nature of members of above mentioned "bands" was proposed by authors of the experimental method described here.

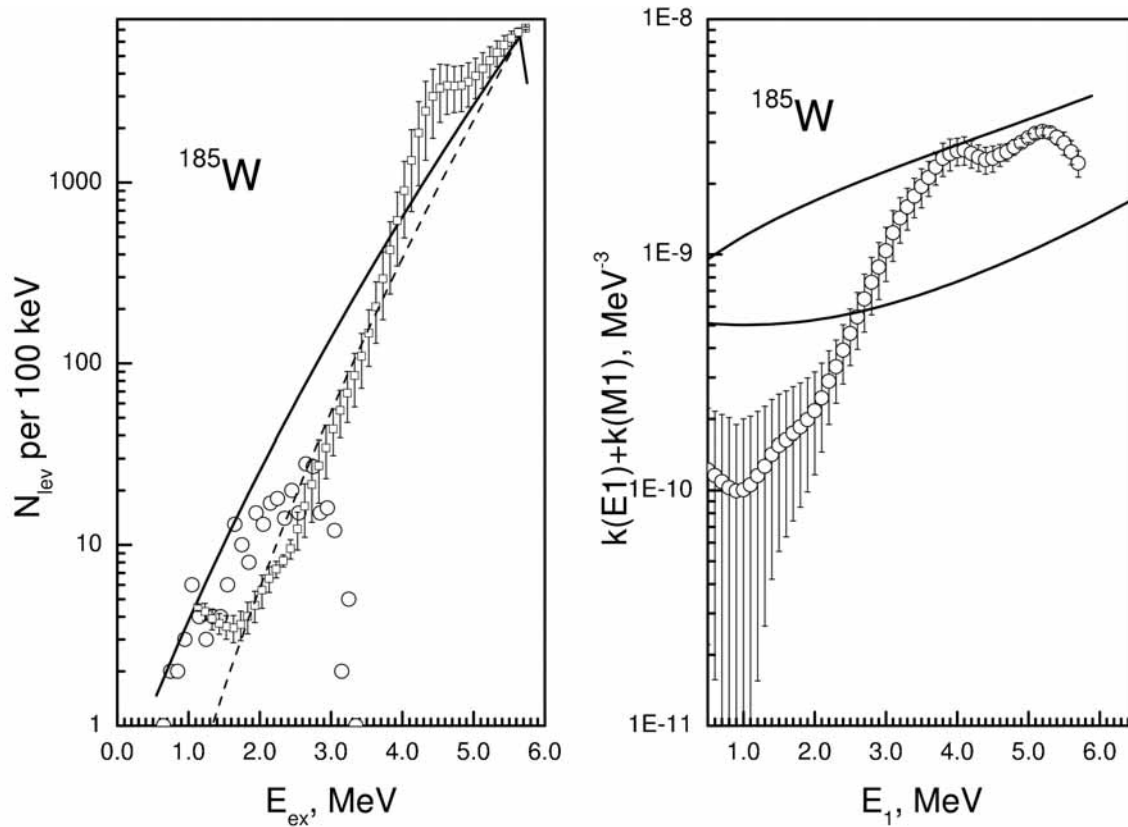


Fig. 2. Left panel: the number of levels of both parities with errors (circles with bars). The upper and lower curves represent predictions of the back-shifted Fermi-gas model and Generalized model of superfluid nucleus in adiabatic approach, respectively. Circles represent the observed number of intermediate levels of the resolved cascades. Right panel: the sum of the probable radiative strength functions of E1 and M1 transitions (with estimated errors). The upper and lower solid curves represent predictions of the Giant Electric Dipole resonance model with constant and depending on quantum energy and nuclear temperature width, respectively (in sum with the value  $k(M1)=const$ ).

And just accounting for the co-existence and interaction of quasi-particle and vibrational types of excitations allows us to give a preliminary and probabilistic picture of the  $\gamma$ -decay process occurring in different nuclei in the excitation energy region up to  $\cong B_n$ :

- (a) the properties of levels below  $\cong 1$  MeV in odd-odd and/or even-odd nuclei and below  $\cong 2$  MeV in even-even nuclei are mainly determined by quasi-particle and vibrational types of excitations;
- (b) the structures of states below  $\cong 3-4$  MeV are under dominant influence of vibrational-type excitations (the energy of phonon equals several hundreds keV);
- (c) re-distribution of the energy to vibrational excitations decreases the total energy of quasi-particle excitations and density of levels of corresponding type below  $\approx 3-4$  MeV;
- (d) above the excitation energy of about 3-4 MeV, deformed nuclei are characterized by sufficiently sharp transition to the states whose peculiarities are determined by inner (quasi-particle) excitations;

These results and following from them conclusions together with other results of extensive study of two-step cascade spectra for many heavy deformed nuclei make extremely important the repetition of this investigation for many compound-states of neutron resonances with known  $J_\pi$  and different  $\Gamma_n^0$  values in both stable and fissile target nuclei.

Analysis of connection between the volume of the obtained information and parameters of the used spectrometers of  $\gamma - \gamma$  coincidences allows estimation of the efficiency of HPGe detectors that is necessary for successful solution of this task - it should be not less than 80-100%.

If indications for deviations from standard statistical model are confirmed for many compound states this will be very serious challenge for modern nuclear model and good basis for its improvement.

1. E. Vasilieva, A. Sukhovej and V. Khitrov, \it Physics of Atomic Nuclei\ 64(2) 153 (2001).\
2. W. Dilg, W. Schantl, H. Vonach and M. Uhl, \it Nucl. Phys\ A217 269(1973).\
3. A. Ignatyuk, Proc. of IAEA Consultants Meeting on the use of Nuclear Theory and Neutron Nuclear Data Evaluation (Trieste, 1975) IAEA-190, Vol. 1, 211 (1976).\
4. A. Ignatyuk, Report IAEA INDC-233(L), IAEA, Vienna.\
5. E. Rastopchin, M. Svirin and G. Smirenkin, \it Yad. Fiz. 52, 1258 (1990).\
6. J. Bardin, L. Cooper and J. Schriffer, \it Phys.Rev. 108 1175 (1957).\
7. A. Sukhovej and V. Khitrov, \it Izv. RAN, Ser. Fiz. 61(11) 2068 (1997).\

## **7. Measurements of the $(n,\alpha)$ cross sections**

### **7.1. Introduction**

IREN will be one of the best neutron sources for astrophysics problems. We are most interested in measuring  $(n,p)$  and  $(n,\alpha)$  cross sections of interest to astrophysics. Initial results from our new program of  $(n,\square)$  experiments at IBR-30 FLNP JINR and ORELA (Oak Ridge, USA) are very encouraging and indicate that a sustained program of  $(n,\alpha)$  measurements should lead to a global improvement in  $\square$ -particle reaction rates for supernova and other explosive nucleosynthesis applications. New  $(n,\square)$  experiments at IREN will help to improve models for supernovae and massive stars, and in the interpretation of observations made with  $\gamma$ -ray telescopes and of isotopic anomalies found in some meteorites.

At the Frank Laboratory of Neutron Physics, JINR, we pioneered the measurement of the  $\alpha$ -particle widths of neutron resonances for intermediate and heavy nuclides. The new experimental challenge is to measure these small cross sections across a broad enough energy range to be useful for astrophysics applications. Therefore, the new IREN measurements covering a wider neutron energy interval are very important. We intend to use the intense flux of epithermal ( $\approx 0.5$  eV to 100 keV) neutrons at the FLNP Neutron Source IREN to perform world-class experiments in nuclear astrophysics, and basic and applied nuclear physics.

### **7.2 Nuclear Astrophysics**

Nuclear reactions involving neutrons play vital roles in many astrophysical scenarios. For example, virtually all elements heavier than iron were made in environments inside stars and supernovae where neutrons interactions dominate the nucleosynthesis. In addition, many of the most interesting new results from the latest generation of astronomical observatories, and from measurements of isotopic anomalies in meteorites, are providing views of the results of this



nucleosynthesis with unprecedented detail and precision. Furthermore, more realistic models of stars and supernovae, made possible by recent advances in computers, are providing new insights into the inner workings of these objects, as well as contributing new insights into related topics such as galactic chemical evolution, and the formation and age of our solar system. However, further progress in these areas is hampered by the lack of accurate rates for the nuclear reactions governing the nucleosynthesis. These astrophysical reaction rates can be determined by measuring neutron-induced cross sections in the energy range between approximately 1 eV and 100 keV.

In some cases it is possible to identify a key reaction or two that need to be measured to elucidate a particular astronomical observable or to test a facet of an astrophysical model. However, in most cases, progress in nuclear astrophysics requires more global improvements in the nuclear data. For example, reaction rate measurements are urgently needed for radioactive isotopes and for stable isotopes of very low natural abundance, for low neutron energies, and for isotopes with small cross sections. Very few of these types of measurements have been made.

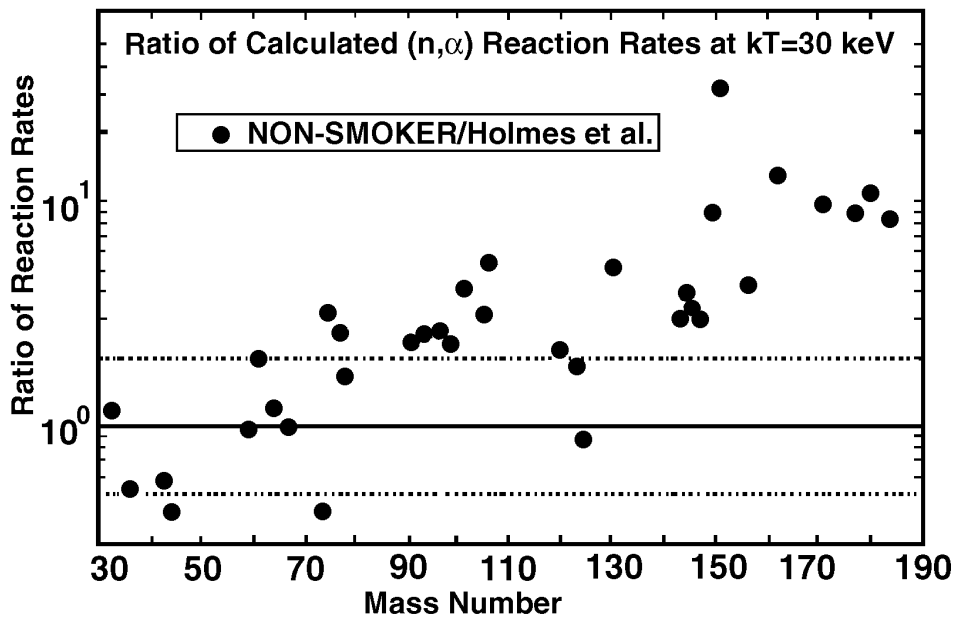


FIG. 1. Ratio of  $(n, \alpha)$  reaction rates at  $kT=30$  keV calculated with two different statistical models, versus mass number. Shown are ratios of rates calculated with the NON-SMOKER code [1] to those calculated by Holmes *et al.* [2] for the 30 nuclides that should be accessible to measurements.

An examination of the observed elemental abundances in the solar system, together with rudimentary nuclear physics considerations, reveals that there were three main processes responsible for the origin of the elements heavier than iron. Almost all these elements are thought to have been synthesized inside stars, supernovae, or other more exotic environments through a chain of neutron capture reactions followed by  $\beta$  decays during the so-called slow neutron capture (or “*s*”) and rapid neutron capture (or “*r*”) processes. The *s* and *r* processes are each responsible for roughly half of the observed heavy element abundances. The remaining neutron-deficient isotopes that cannot be reached via neutron capture pathways are thought to have been formed in massive stars or during supernova explosions through the photodissociation, (or “*p*”) process. Little is known about the details of the origin of the proton rich isotopes of the intermediate and heavy elements (the so-called *p* isotopes  $^{92}\text{Mo}$ ,  $^{96}\text{Ru}$ ,  $^{102,106,108}\text{Pd}$ ...). In general, the *p* isotopes are thought to be produced during stellar explosions (in novae and/or supernovae), either through a series of photodisintegration reactions starting from seed material built up during previous nucleosynthesis processes, or through a chain of charged particle capture reactions on lighter elements. However, the detail of how and where the *p* nuclei are synthesized are very uncertain. A better understanding

of their origin should lead to better models of novae and supernovae explosions and would also impact related areas such as the origin of isotopic anomalies in meteorites and the formation of the solar system.

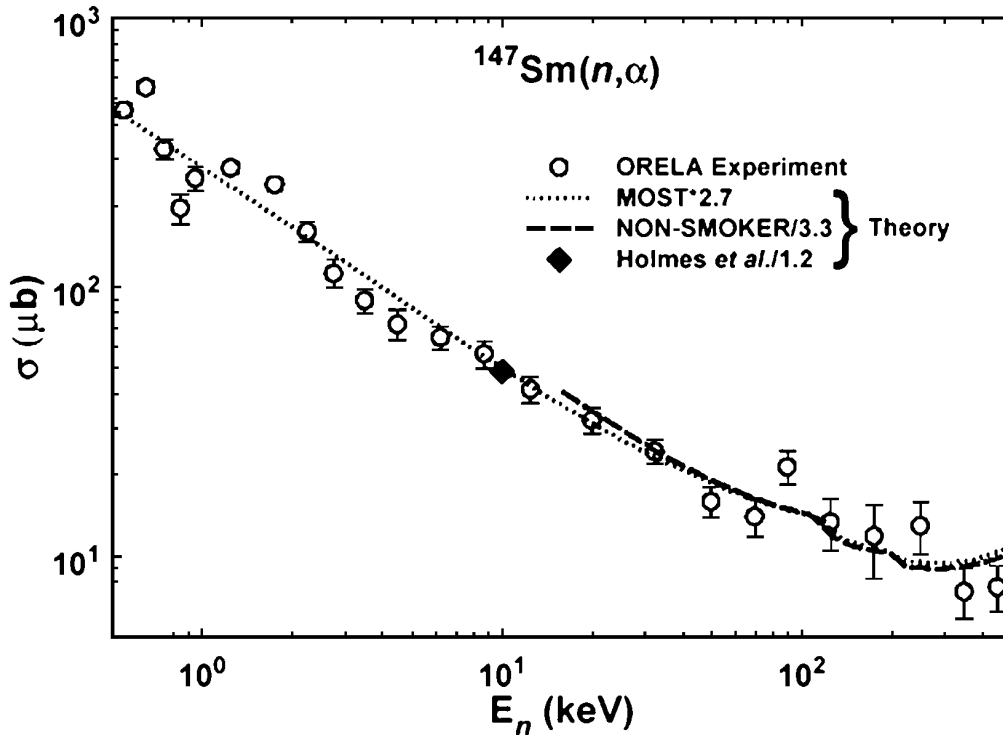


FIG. 2. Cross sections for the  $^{147}\text{Sm}(n, \alpha)$  reaction. Shown are the measurements [3] (circles) and calculations by Holmes *et al.* [2] (diamonds), as well as calculations using the newer statistical model codes NON-SMOKER [1] (long-dashed curve), and MOST [4] (dotted curve). Note that the theoretical calculations of Refs. [1,2,4] have been normalized by the factors given in the legend.

A large part of the uncertainty regarding the origin of the  $p$  isotopes is due to the fact that most the rates for the nuclear reactions governing the nucleosynthesis flow which produced these nuclides are poorly constrained. In particular,  $(\gamma, \alpha)$  and  $(p, \alpha)$  reactions constitute some of the most important links in the nucleosynthesis chain thought to be responsible for their origin. However, it is very unlikely that the rates for these reactions will be determined by direct experiments and they are also currently very poorly constrained by theory (because of our poor knowledge of the  $\alpha$ -nucleus optical potential, which forms a crucial part of the nuclear statistical model used to calculate these rates).

The uncertainties in the  $(\gamma, \alpha)$  and  $(p, \alpha)$  reactions rates could be reduced considerably by making a series of  $(n, \alpha)$  measurement at IREN. We have compared calculated cross sections from the updated, state-of-the-art statistical model code “Non-Smoker” [1] to previous calculations [2]. The result, shown in fig.1 reveal a systematic difference between the new and older calculations. This comparison between calculated cross sections indicates that  $(n, \alpha)$  measurement will be sensitive to the poorly constrained  $\alpha$ -nucleus optical potential, hence, to reduce the uncertainties in explosive nucleosynthesis calculations.

The  $^{147}\text{Sm}(n, \alpha)$  experimental cross section data [3] are shown in fig.2.

Both  $(n, \square)$  and  $(n, \square)$  measurements are needed. Only a very few  $(n, \square)$  measurements have been made, and they indicate that the reaction rates used in  $p$  process models are in error by large factors; hence, there is much room for improvement. So far, none of these reaction rates have been measured across the range of temperatures needed by the models. It should be possible at the IREN to measure many important samples. The large flux at the IREN should make possible for the first

time ( $n, \square$ ) measurements on many radioisotopes of interest to the  $r$  and  $p$  processes. Also, there are a few radioisotopes of lighter elements for which ( $n, p$ ) and/or ( $n, \square$ ) reaction rates are needed.

### 7.3 Nuclear Physics

Research in basic nuclear physics will concentrate on measurements of the violations of fundamental symmetries and related topics. Pioneering work in these areas has been carried out by groups working at the IBR-30 FLNP. The substantial boost in flux at the IREN compared to this facility will make possible the next generation of experiments in these areas.

According to modern theoretical conceptions (see [5] and references therein) the N. Bohr's compound state of nucleus may be viewed as a typical representative model of the quantum chaos. If it is so, the neutron spectroscopy must be a powerful tool for the investigation of the main properties of the quantum chaos. It is well known, the description of the neutron resonances by the pure statistics theory ("black" nucleus theory) is not correct.

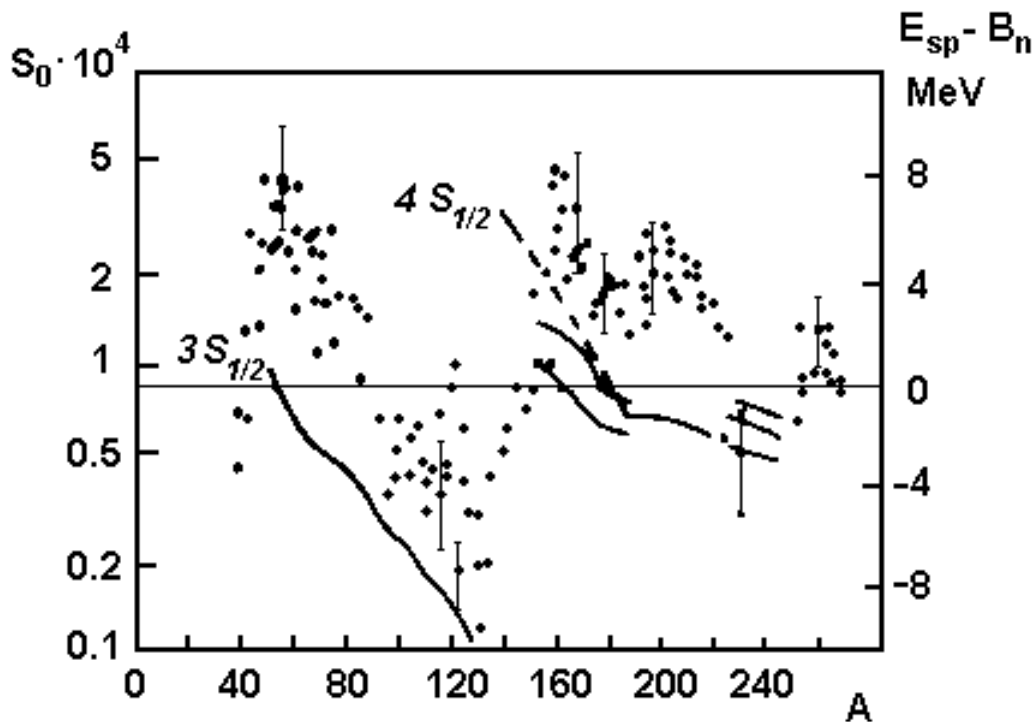


Fig.3. Dependences on atomic weight,  $A$  of the  $s$ -wave strength functions,  $S_0$  (points) and of the distances between single particle shell position,  $E_{sp}$  and  $B_n$  values (curves).

The neutron strength functions  $S_0$  are not constant, as they must be according to the black nucleus theory ( $S_0=10^{-4}$ ), but the variations of  $S_0$  values from one nucleus to another are very well reproduced by the optic (semitransparent) model of nucleus. This model takes into account the essential single-particle component contribution to the neutron resonances wave function. Good correlation of the  $S_0$  values and the proximity of the single-particle shell position to the neutron binding energy  $B_n$  of the nucleus for all atomic nucleus weights is illustrated by Fig.3. At the same time the quantum chaos may be distorted not only by the single-particle component contribution but by the many quasi-particle component contribution too. But this contribution practically has not been investigated experimentally up to now. The main cause of this situation is that the usually investigated neutron reactions did not directly depend on the many quasi-particle wave function components. The only type of an experiment, which must be productive is the ( $n, \alpha$ ) reaction investigations with resonance neutrons. Unfortunately the cross sections of this reaction are very small according to the small Coulomb barrier penetrability for  $\alpha$ -particle.

The main experimental results in the ( $n, \alpha$ ) reaction investigation were obtained on the high intensity neutron spectrometers - pulsed reactor IBR-30 and ORELA (ORNL, Oak Ridge) for

middle and heavy nuclei [6,7], and on the GELINA-spectrometer of neutrons [8] and Los-Alamos proton LINAC [9] for light nuclei. Unfortunately, the poor neutron energy resolution of Dubna spectrometer, the lack of fast  $\alpha$ -particle detectors with a big area sample in Geel and the lack of long flight paths in Los Alamos gave no possibility to investigate many dozens of the neutron resonances for an individual nucleus and to make statistical analysis of the  $\alpha$ -particle strength functions  $S_\alpha$ .

Nevertheless the analysis of the experimental data for  $^{147}\text{Sm}$  resonances [11], is giving the evidence for a possible energy dependence of the  $S_\alpha$  values for energy bins 200-500 eV ( $\sim 20$ -50 resonances). This result presented by Fig.4. is contradicted to the statistics theory. On increasing of  $S_\alpha$  values indicate and last measurement of this reaction in ORNL [12].  $\chi^2=2.1$  for  $S_\alpha = \text{const}$  and  $\chi^2=1.2$  for  $S_\alpha \sim E_n$  for neutron energy interval up to 700 eV. For more extensive interval (up to several tens of keV) this non-statistical effect may be investigated on IREN facility by measurement of average over resonances cross section of  $(n,\alpha)$  reaction. And maybe it will confirm that the many quasi-particle component of the wave function is influence on the neutron cross sections. According to the calculation in the framework of quasi-particle phonon model by V.G. Soloviev's group, the distance between the four quasi-particle "shells" for this atomic weight region is about several keV (fig.4).

For many light and near magic nuclei, where the distances between resonances are large, a noticeable contribution can also come from interresonance cross sections that are poorly measured by TOF technique in many cases. In some times interresonance effects can substantially change the picture. As an example for the possible important role of interresonance interference effects, we cite the following case. Measuring the thermal cross section of the  $(n,\alpha_1)$  reaction on  $^{145}\text{Nd}$  and  $^{67}\text{Zn}$ , Ashgar and Emsallem [13] very well coincide with value calculated from the parameters of individual resonances [14], whereas for the  $(n,\alpha_0)$  reaction the measured cross section [13] appeared an order of magnitude less than that calculated by the parameters of [14]. The analysis of the situation [15] suggests that the reason for the discrepancy of the results could be a specific interresonance interference. The nature of this specific effect (how much resonances take part in this effect, for example) may be investigated on IREN facility.

Very surprised preliminary results were demonstrated in [15]. According to fig. 5 [16] the average value  $\langle \Gamma_\alpha(J^\pi=3^-) \rangle$  is twice smaller than value  $\langle \Gamma_\alpha(J^\pi=4^-) \rangle$  for  $E_n > 300$  eV although according to theory this relation must be reverse so long as  $\alpha$ -transitions for resonances  $J^\pi=4^-$  to the ground state  $J^\pi=0^+$  are forbidden by parity conservation whereas for resonances  $J^\pi=3^-$  are not, and must be 5 – 10 times larger as it is for  $E_n < 300$  eV according to fig.5 [16] and old Dubna experiment [6]. This result may be caused by mistake in resonance spin identification, used by authors [16]. Measurements of  $\alpha$ -particle spectra in resonances, planned on IREN, may give the real explanation of this problem.

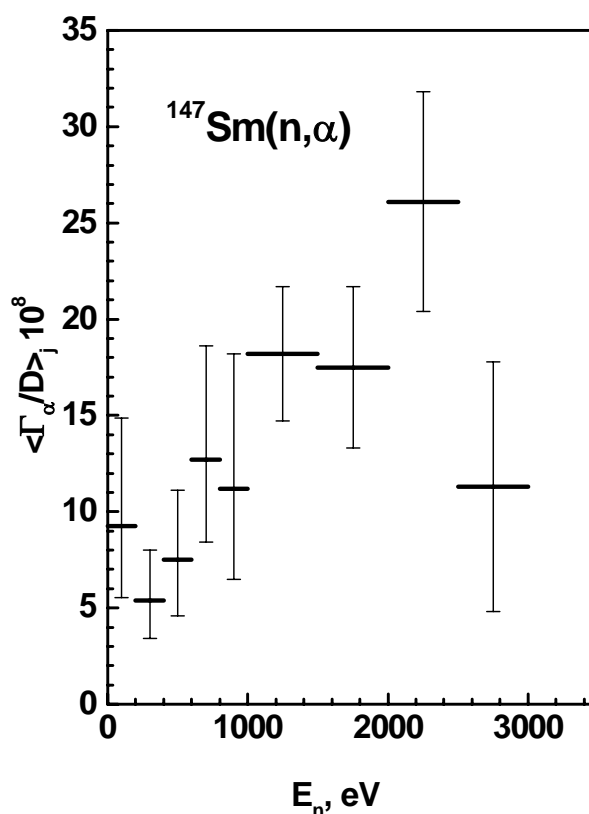


Fig.4. Variability of the  $\alpha$ -particle strength functions,  $S_\alpha$  of  $^{147}\text{Sm}$  isotope for different energy bins.

## 7.4 Experimental Approach

A well collimated, well shielded beam line viewing the water moderator at the IREN will be required to carry out this research. The  $(n,p)$ , and  $(n,\square)$  measurements for astrophysics and applied physics will require sophisticated ion chambers and electronics and/or solid-state detectors. The basic nuclear physics experiments will require an automated sample changer and an efficient neutron detector at a flight path distance on the order of 10-85 m. The capital repairs of 10, 20, 30 and 85 meter path of flight of beam-line 1 is necessary.

Team members from Dubna, Lodz, ORNL and NUM are experts in designing, constructing and using ionization detectors for charged particles at white neutron sources. It is expected that students from collaborating universities will make substantial contributions to this effort. Many of the anticipated experiments, which we estimate would take one to two weeks to finish, would make excellent dissertation topics.

The ionization chambers and their associated electronics should require about \$100k. The main problem will be sample preparation (purchase).

- 1) R.D. Hoffman, S.E. Woosley, T.A. Weaver, T. Rauscher, and F.-K. Thieleman, *Astrophys. J.* **521**, 735 (1999).
- 2) J.A. Holmes, S.E. Woosley, W.A. Fowler, and B.A. Zimmerman, *At. Data Nucl. Data Tables* **18**, 305 (1976).
- 3) S.E. Woosley, W.A. Fowler, J.A. Holmes, and B.A. Zimmerman, *At. Data Nucl. Data Tables* **22**, 371 (1978).
- 4) S.Goriely, in *Nuclei in the Cosmos*, ed. by N.Prantzos and S.Harrissopoulos (Edition

- Frontieres, Gif-sur-Yvette, 1998), p. 314.
- 5) V.E.Bunakov, F.F.Valiev, Yu.M.Chuvilsky, Phys.Lett. **A243** (1998) 288
  - 6) N.P.Balabanov, V.A.Vtyurin, Yu.M.Gledenov, Yu.P.Popov Sov.J.Part. Nucl. **21**(1990) 131
  - 7) Yu.M.Gledenov, P.E.Koehler, J.Andrzejewski, K.Guber, T.Rausher.  $^{147}\text{Sm}(n,\alpha)$  cross section measurements from 3 eV to 500 keV: Implications for explosive nucleosynthesis reaction rates. Phys. Rev. **C62** (2000) 042801.
  - 8) Wagemans C., Schillebeeckx P., Weigmann H., Druyts S., In: "Capture Gamma- Ray Spectroscopy and Related Topics", Ed. J. Kern, World Sci., Singhapore, (1994) 638
  - 9) Koehler P.E., Graff S.M., O'Brien H.A., Gledenov Yu.M., Popov Yu.P., Phys. Rev.C, **47** (1993) 2107
  - 10) A.Antonov, Yu.M.Gledenov, S.Marinova, Yu.P.Popov, J.Rigol, Sov.J.Nucl.Phys. **39** (1984) 794
  - 11) Yu.P.Popov, In: "From Spectroscopic to the Chaotic Feature of Nuclear Systems", ed. by D. Seeliger, World Scientific, Singapore, 1992, p.34.
  - 12) Yu.M.Gledenov, P.E.Koehler, J.Andrzejewski, Yu. P. Popov, R.Yu. Gledenov. " $^{147}\text{Sm}(n,\alpha)$  Cross Section Measurements from 3 to 500 keV: Resonance Neutrons. In: Proc.of Intern.Conf. on Nuclear Data for Science and Technology (ed. K.Shibata) October 7 – 12, 2001. V.1, p.358-361.
  - 13) Emsalem, A. and Asghar, M., *Z. Phys.* **A275**,(1975) p. 157.
  - 14) Popov, Yu.P., Pshitula, M., Rodionov, K.G., *et al.*, *Yad.Fiz*, vol. 12., (1971) p. 913.
  - 15) Vtyurin, V.A., Zhak, A., Popov, Yu.P., and Ukraintsev, V.F., *Yad. Fiz.*, vol. 45,(1986) p. 1292.
  - 16) P.E.Koehler, Yu.M.Gledenov, "Evidence for non-statistical effects in  $^{147}\text{Sm}(n,\alpha)$ ." (Unpublished).